Surface carrier transport in Y nanojunctions: Signatures of the geometric potential

Giampaolo Cuoghi,[1,2,*] Giulio Ferrari,[1,3] and Andrea Bertoni[1]
[1]*CNR-INFM-National Research Center on Nano-Structures and Bio-Systems at Surfaces (S3), Via Campi 213/A, 41100 Modena, Italy*
[2]*Dipartimento di Fisica, Università degli Studi di Modena e Reggio Emilia, 41100 Modena, Italy*
[3]*CNISM, Unità di Ricerca di Modena, 41100 Modena, Italy*
(Received 20 January 2009; published 25 February 2009)

The effective potential originated by the nonplanar geometry of a two-dimensional electron gas (2DEG) modifies its coherent transport properties. To date no direct evidence of such purely geometric potential has been revealed. Here we expose its effects by computing the transmission characteristics of a semiconductor cylindrical 2DEG forming a Y junction. For some cylinder radii, we find that the activation thresholds of the transmission channels in the two drain leads are exchanged, with this effect being robust against the geometrical details of the three-terminal junction.

DOI: 10.1103/PhysRevB.79.073410 PACS number(s): 73.23.Ad, 73.63.Fg, 68.65.−k, 03.65.−w

Low-dimensional semiconductor heterostructures have long been a key system both for novel nanoelectronic devices and for probing the quantum effects of carrier dynamics. In particular, high-mobility two-dimensional (2D) electron gases (2DEGs) are being routinely fabricated in many advanced laboratories;[1] usually, they have a planar configuration, with the carriers constrained in the lower quantum-confined states in a given direction and free to move along the two perpendicular directions. Recently, a number of nonplanar 2DEG structures have been proposed and fabricated within semiconductor technology.[2] For example, cylindrical 2DEGs (C2DEGs) have been obtained by rolling-up mismatched semiconductor layers[3,4] or by employing self-standing semiconductor nanowires as substrates for an epitaxial overgrowth of different semiconductor shells.[5] This latter technique appears to be more promising, given the absence of structural defects and the possible use of branched nanowires.[6,7] Epitaxial overgrowth of such wires may lead to C2DEG Y junctions or more complex curved 2D structures.

Understanding charge transport in these structures is not only of practical importance for their possible applications but also of fundamental interest to shed light on a number of general nontrivial quantum effects brought about by the shape of the system itself. In fact, the equation of motion of a two-dimensional system that is bent into the third spatial dimension has many similarities to the dynamical law proper of a non-Euclidean multidimensional space, as emerging in general relativity.[8]

We follow the procedure described in Refs. 9 and 10 and obtain the following Hamiltonian for a particle bound to a curved surface (not including external fields[11]):

$$-\frac{\hbar^2}{2m}\sum_{i,j=1}^{2}\frac{1}{\sqrt{G}}\partial_i[\sqrt{G}(\mathbf{G}^{-1})_{ij}\partial_j]-\frac{\hbar^2}{2m}[M^2-K], \qquad (1)$$

where the two subscripts i and j indicate the two coordinates tangent to the surface and the matrix $\mathbf{G}$ is the metric tensor of the surface, with G representing its determinant. The first term of Eq. (1) is the usual Schrödinger kinetic operator for curvilinear coordinates. The second term has the form of an effective potential arising from the mean and Gaussian curvatures, M and K, respectively. Its presence originates different carrier states with respect to the ones obtained through a standard 2D model. While this topic has a rather long history,[12–14] the question of the proper theoretical approach and of the possibility to experimentally reveal the above curvature-induced geometric potential (GP) is very topical mainly due to the recent development of the nanostructures mentioned above.

In this work, we show that the coherent transport characteristics of a three-terminal device consisting of a Y junction (Fig. 1) of three C2DEGs can expose the existence of the GP. To this aim, we solve numerically the open-boundary quantum dynamical equation for a carrier lying on the curved surface and injected from one of the branches. For different injection energies we compare the coherent transmission coefficients in two cases, namely, as obtained from (a) Eq. (1), which includes the GP, and (b) the same equation without the second term, i.e., as derived from a 2D Lagrangian approach,[12] discretized on the Y-junction surface. In the following we indicate as "with GP" and "without GP" the two cases (a) and (b), respectively. To compute the scattering

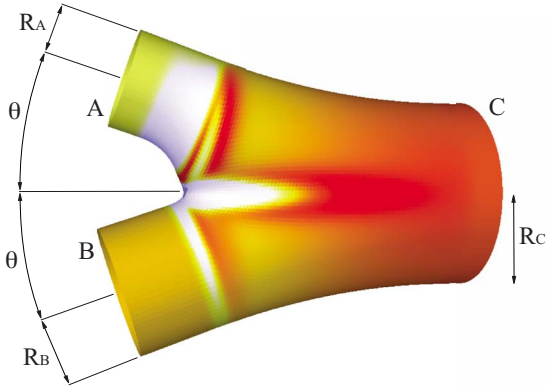

FIG. 1. (Color online) Y junction of the three cylinders connected by a smooth surface. In the numerical simulations the following values have been taken for the radii: $R_A=15$ nm, $R_B=20$ nm, and $R_C=30$ nm. A and B cylinders form an angle $\theta=\pi/10$ with C, and the effective mass for GaAs $m=0.067m_e$ has been used. The GP is represented in color code on the surface, with values ranging from zero (darker color) to about −30 meV (lighter color).

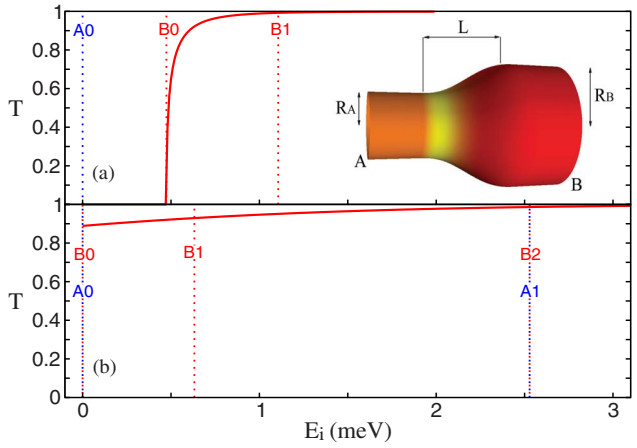

FIG. 2. (Color online) Quantum transmission probability for a single cylindrical junction (shown in the inset with the GP in color code) with $R_A=15$ nm, $R_B=30$ nm, and $L=50$ nm. The carriers are entering the device in the ground transverse mode of cylinder A, with a kinetic energy E_i. The vertical dotted lines indicate the energies of the modes in A and B, as obtained from Eq. (2). **A***n* (**B***n*) is the nth transverse mode in the C2DEG $A(B)$. Panels (a) and (b) represent the results of the simulations with and without the GP, respectively.

states, we adopt a real-space finite-difference approach and include the leads through the *quantum transmitting boundary method*.[15]

Before tackling the Y-junction system, we briefly investigate a simpler yet illustrative case, namely, a single junction of two C2DEGs with different radii, $R_A<R_B$. By specifically solving Eq. (1) for a cylinder with radius R, we obtain the following energies for the transverse modes $n=0,1,2,\ldots$ of the leads:[16]

$$E_n = \frac{n^2\hbar^2}{2mR^2} - \frac{\hbar^2}{8mR^2}, \tag{2}$$

with $n=0$ labeling the ground state. The first term of the above equation represents the eigenenergies of a particle on a one-dimensional (1D) ring, while the second term is the GP. It is easy to see that on the cylinders the GP is always negative and constant, as in these regions the surface curvature only depends on R. Thus, the presence of the GP does not change the character of the transmission channels but acts solely as a constant shift on their activation energies. Specifically, the smaller the radius, the more negative the GP. In our model the two cylinders are connected by a smooth surface of length L, as shown in the inset of Fig. 2 where the GP is also represented in color code on the surface; darker color means less negative GP. The dimensions used in the simulations are indicated in the caption.

We consider an electron injected in the ground mode of the smaller-radius cylinder A, with different values for the longitudinal kinetic energy E_i. Figures 2(a) and 2(b) show the transmission probability of the above structure with and without the GP, respectively, as a function of E_i. The dotted vertical lines indicate the transverse-mode energies of the two leads A and B, as indicated by their labels, **A***n* and **B***n*, respectively.

The most evident feature is the complete reflection occurring at low injection energies when the GP is included. In fact, as explained above, the different surface curvatures of the two cylinders shift their transverse energies. In particular, the ground mode of cylinder B acquires an energy almost 0.5 meV larger than the ground state of cylinder A. This is not the case when the GP is not considered, as shown in Fig. 2(b) where the ground channels of A and B are degenerate. Note that such a degeneracy (lifted by the GP) is due to the periodic boundary conditions of the transverse modes and only holds for the $n=0$ ground states, as one can see from Eq. (2). This degeneracy is typical of systems in which the carriers are confined on a cylindrical-like surface, as the energy of the transverse ground state is independent of their dimension.

The low-energy suppression of the transmission described above represents a manifestation of the GP and is at the base of our results. However, a clear unambiguous experimental evidence of such a behavior in a two-terminal system would be quite difficult mainly due to the difficulty in ascribing a specific value of the transmission threshold to a particular effect. In fact, the presence of impurities in the sample, the lack of a perfect control on the local electric field along the device, or the unknown effect of the contacts could induce a similar result. What is needed is a *qualitative* change in the transport characteristics rather than a *quantitative* shift. In the following, we show how a Y-junction system can reveal a true signature of the GP.

The structure under consideration is depicted in Fig. 1. It consists of a Y junction of three C2DEGs A, B, and C, connected by a smooth surface. The cylinder radii are $R_A<R_B<R_C$, with the specific values reported in the figure caption. Figure 1 also reports in color code the value of the GP on the surface. It is easy to identify the three areas in which the GP is particularly attractive, namely, the light regions close to the saddle points, where the surface has opposite curvatures along two perpendicular directions. This can be also deduced by the expression for the GP given in Eq. (1). Although the coherent scattering of the injected carriers is governed by the spatial modulation of the GP inside the Y junction, we found that the qualitative behavior of the transmission is rather insensitive to the geometrical details of the junction,[16] as we substantiate later.

We first consider a carrier injected in the ground channel of C2DEG A and compute the transmission (and reflection) coefficients in the different modes of the three branches. The transmission probabilities in B and C as a function of the injection energy are shown in Figs. 3(a) and 3(b), with and without the GP, respectively.[17]

In the former case (a) the GP generates a shift of the transverse modes as in the two-terminal system described above. In particular, the ground mode in B (**B**0) is activated at about 0.3 meV, while that in C (**C**0) is activated just before 0.5 meV. This is very different from the case (b) with no GP, where the ground channels of both B and C are always open so that the carriers are never fully reflected. At low injection energies, we point out another important difference between the two cases; the transmission in the larger cylinder C is higher than in the smaller cylinder B when the

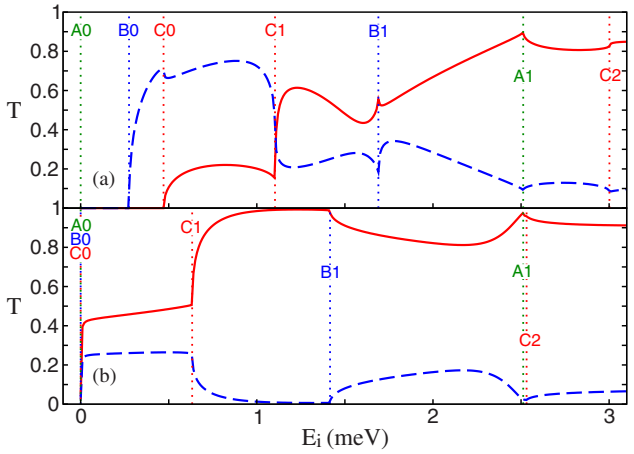

FIG. 3. (Color online) Quantum transmission probabilities for the Y junction of Fig. 1 as a function of the kinetic energy E_i (a) with and (b) without the GP. The carriers are entering the device in the ground transverse mode of branch A and are transmitted in B (dashed line) or in C (solid line). The vertical dotted lines indicate the energies of the modes in A, B, and C, as explained in the main text.

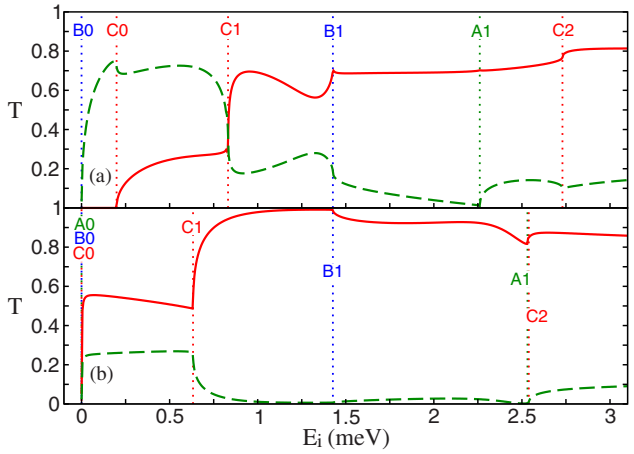

FIG. 4. (Color online) Same as Fig. 3 but with the carriers entering from cylinder B and transmitted in A (dashed line) or C (solid line). Again, panels (a) and (b) show the results with and without the GP, respectively.

GP is not considered, while the opposite holds when the GP is included, as can be seen from Figs. 3(a) and 3(b). Indeed, the above effect is rather surprising and only due to the GP that lowers the $n=0$ transverse-mode energy in B with respect to the same mode in C. As we increase further the injection energy, we reach the first-excited transverse mode in C, labeled as **C**1 in Fig. 3, which has a lower energy than **A**1 and **B**1, due to the smaller radii of cylinders A and B. By comparing the two panels of the above figure, it is clear that the inclusion of the GP increases the energy of **C**1 of about 0.5 meV and, similarly, that of **B**1 of 0.3 meV. However, it is important to stress here also that without the GP, the excited modes in the three cylinders are not degenerate, contrary to the $n=0$ modes. Besides the above energy shift of the modes, another important difference between Figs. 3(a) and 3(b) is evident when the **C**1 mode comes into play, opening a second outgoing channel in C2DEG C. While in (b) the transmission in C remains above that in B and almost reaches one, in (a) the two transmission probabilities cross. After the crossing, C remains to be the favored outgoing channel in both cases (a) and (b).

Figure 4 reports the transmission coefficient for the Y junction described above when the electrons are injected from branch B. Contrary to Fig. 3, the carrier is never totally reflected. In fact, the GP in A is lower than in the entering branch B; thus the channel **A**0 is always available. Apart from this effect, the behavior of T is similar to the previous case, with the crossing of the two coefficients only present when the GP is accounted for. This confirms that the effect of the GP just described is rather robust against the variation in the C2DEG diameters, as far as the ones of the two outgoing branches are significantly different. Also, it does not arise from the details of the coherent scattering inside the Y junction (even though the Y shape of the system enhances the effect), rather it is related to the peculiar effect of the GP on the transverse modes with periodic boundary conditions. In order to verify this, a number of Y junctions with different shapes but the same cylinder radii has been analyzed, leading to very similar results (not reported here for the sake of brevity).

Now we show that the crossing of the two transmissions induced by the GP should be detectable in a transport experiment. We consider three leads connected to the C2DEGs, which are made of the same material and with the bottom of their conduction band equal to the lower transverse energy of the cylinders plus their GP. This configuration corresponds to three GaAs-based planar 2DEGs, acting as leads for the device. The two drain leads attached to cylinders B and C are kept at the same potential $\mu_B=\mu_C$, while the potential of the source lead, connected to A, is $\mu_A=\mu_B+e\Delta V$, with the volt-

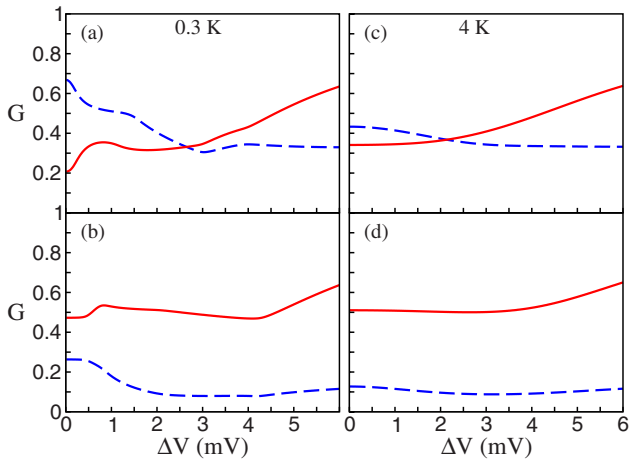

FIG. 5. (Color online) Conductance, in units of $\frac{2e^2}{h}$, between leads A and B (dashed line) and between leads A and C (solid line) for the Y-junction system of Fig. 1. G is reported as a function of the applied bias between A and the other two leads, always at the same potential. Panels (a) and (b) show the results with and without the GP, respectively, for a temperature of 0.3 K. Panels (c) and (d) show the same at 4 K. The two coherent conductances cross only when the GP is included in the simulations.

age drop ΔV equally split between the two connections.[18] Since the different behavior of the transmission coefficients, with and without the GP, is prominent at low energies, we need to take a low Fermi level in the leads in order to expose the above differences. Specifically, we use a Fermi energy of 0.4 meV above the bottom of the conduction band of the 2DEGs. Charge effects inside the Y device are not considered due to the very low density of the carriers. In Fig. 5 we report the *A*-*B* (dashed line) and *A*-*C* (solid line) conductances as a function of the applied voltage bias ΔV. The results are obtained by using the Landauer-Büttiker approach for a three-terminal device.[18] Two different temperatures are considered in the left and right graphs, namely, 300 mK and 4 K, respectively.

The plots show clearly that a crossing in the *A*-*B* and *A*-*C* conductances represents a signature of the GP. In fact, when the GP is not taken into account (lower plots in Fig. 5), i.e., when a standard Schrödinger equation is adopted to compute the current-carrying states, the current in the *C* lead is always larger than that in the *B* lead, as expected due to the difference in their density of transverse states. On the other hand, when the GP is included (upper plots in Fig. 5), the crossing between the transmission probabilities reported in Fig. 3 gives rise to a corresponding crossing between the conductances that, although less pronounced, should be detectable experimentally.

In conclusion, we showed how the study of coherent electron dynamics in Y junctions of C2DEGs is able to reveal the presence of the GP and to expose the soundness of one of the theoretical approaches proposed to obtain the single-particle Hamiltonian in curved space. The experimental test proposed here could show that alternative theoretical derivations[12] not leading to a GP term are not suitable for the description of the quantum carrier dynamics on curved 2D nanostructures.

We thank Fiorenzo Bastianelli and Guido Goldoni for most helpful discussions. This work was supported by FIRB under Project No. RBIN04EY74. A.B. acknowledges INFM Seed Project 2008.

*giampaolo.cuoghi@unimore.it; www.nanoscience.unimore.it

[1] T. Ihn, *Electronic Quantum Transport in Mesoscopic Semiconductor Structures* (Springer, New York, 2004).
[2] We only consider devices fabricated through semiconductor heterostructures as model systems for our simulations. However, graphene also offers many opportunities for curved 2D nanostructures, as spherical fullerenes (Ref. 19), cylindrical carbon nanotubes (Ref. 20), or toroidal nanorings (Ref. 21). Y junctions (Refs. 22 and 23) of carbon nanotubes have also been proposed as novel nanoelectronic devices (Ref. 24).
[3] V. Y. Prinz, V. A. Seleznev, A. K. Gutakovsky, A. V. Chehovskiy, V. V. Preobrazhenskii, M. A. Putyato, and T. A. Gavrilova, Physica E **6**, 828 (2000).
[4] O. G. Schmidt and K. Eberl, Nature (London) **410**, 168 (2001).
[5] A. Fontcuberta i Morral, D. Spirkoska, J. Arbiol, M. Heigoldt, J. R. Morante, and G. Abstreiter, Small **4**, 899 (2008).
[6] D. Wang, F. Qian, C. Yang, Z. Zhong, and C. M. Lieber, Nano Lett. **4**, 871 (2004).
[7] K. A. Dick, K. Deppert, M. W. Larsson, T. Mårtensson, W. Seifert, L. R. Wallenberg, and L. Samuelson, Nature Mater. **3**, 380 (2004).
[8] C. W. Misner, K. S. Thorne, and J. A. Wheeler, *Gravitation* (Freeman, San Francisco, 1973).
[9] H. Jensen and H. Koppe, Ann. Phys. (N.Y.) **63**, 586 (1971).
[10] R. C. T. da Costa, Phys. Rev. A **23**, 1982 (1981).
[11] G. Ferrari and G. Cuoghi, Phys. Rev. Lett. **100**, 230403 (2008).
[12] B. S. DeWitt, Rev. Mod. Phys. **29**, 377 (1957).
[13] T. Kawai, Found. Phys. **5**, 143 (1975).
[14] J. M. Domingos and M. H. Caldeira, Found. Phys. **14**, 607 (1984).
[15] C. S. Lent and D. J. Kirkner, J. Appl. Phys. **67**, 6353 (1990).
[16] A. Marchi, S. Reggiani, M. Rudan, and A. Bertoni, Phys. Rev. B **72**, 035403 (2005).
[17] See EPAPS Document No. E-PRBMDO-79-075907 for two movies showing the time-dependent dynamics of a single-electron wave function injected from cylinder *A*. For more information on EPAPS, see http://www.aip.org/pubservs/epaps.html.
[18] S. Datta, *Electronic Transport in Mesoscopic Systems* (Cambridge University Press, Cambridge, England, 1995).
[19] H. W. Kroto, J. R. Heath, S. C. O'Brien, R. F. Curl, and R. E. Smalley, Nature (London) **318**, 162 (1985).
[20] S. Iijima, Nature (London) **354**, 56 (1991).
[21] H. R. Shea, R. Martel, and P. Avouris, Phys. Rev. Lett. **84**, 4441 (2000).
[22] B. C. Satishkumar, P. J. Thomas, A. Govindaraj, and C. N. R. Rao, Appl. Phys. Lett. **77**, 2530 (2000).
[23] W. Z. Li, J. G. Wen, and Z. F. Ren, Appl. Phys. Lett. **79**, 1879 (2001).
[24] P. R. Bandaru, C. Daraio, S. Jin, and A. M. Rao, Nature Mater. **4**, 663 (2005).